antioxidants

MDPI

Article

Bioactive Properties of Enzymatically Hydrolyzed Mulberry Leaf Proteins: Antioxidant and Anti-Inflammatory Effects

Yichen Zhou [1,†], Tianxu Liu [2,†], Rijun Zhang [1,*], Junyong Wang [1], Jing Zhang [1], Yucui Tong [1], Haosen Zhang [1], Zhenzhen Li [1], Dayong Si [1] and Xubiao Wei [1,*]

[1] Laboratory of Feed Biotechnology, State Key Laboratory of Animal Nutrition and Feeding, College of Animal Science and Technology, China Agricultural University, Beijing 100193, China; yczhou51@alu.cau.edu.cn (Y.Z.); wangjy9722@cau.edu.cn (J.W.); tracey9825@cau.edu.cn (Y.T.); s20223040758@cau.edu.cn (H.Z.); s20223040734@cau.edu.cn (Z.L.); dayong@cau.edu.cn (D.S.)

[2] Beijing Key Laboratory for Animal Genetic Improvement, National Engineering Laboratory for Animal Breeding, Key Laboratory of Animal Genetics and Breeding of the Ministry of Agriculture, College of Animal Science and Technology, China Agricultural University, Beijing 100193, China; liutianx@cau.edu.cn

* Correspondence: rjzhang@cau.edu.cn (R.Z.); weixubiao@cau.edu.cn (X.W.)

† These authors contributed equally to this work.

Abstract

Oxidative stress and inflammatory responses often occur concomitantly, and they are key causative factors in various human and animal diseases. Evidence suggests that mulberry leaf protein (MLP) may have potential antioxidant and anti-inflammatory properties, but there are significant challenges in enhancing their bioactivities. In this study, MLP was enzymatically hydrolyzed using papain, protamex, alkaline protease, trypsin, and neutral protease, followed by comprehensive evaluation of the antioxidant capacity, anti-inflammatory properties, and cytotoxicity of the hydrolysates. Our findings revealed that some enzymes significantly enhanced the peptide production and antioxidant activity of MLP ($p < 0.01$), and its activity was positively correlated with the degree of hydrolysis. Among the five hydrolysates, neutral protease hydrolysate (NeuH) exhibited the best antioxidant properties, with free radical scavenging rates of 71.58 ± 0.42% (ABTS), 26.38 ± 0.15% (OH), and 73.91 ± 0.37% (DPPH) at a concentration of 0.1 mg/mL. In addition, NeuH significantly suppressed IL-6 secretion ($p < 0.01$) and downregulated mRNA expression of IL-6, iNOS, and COX-2 inflammatory markers. This study not only establishes a correlation between enzymatic parameters and MLP biological functions but also demonstrates the potential of optimized MLP hydrolysates, particularly NeuH, as valuable natural antioxidant and anti-inflammatory ingredients for functional foods or nutraceuticals aimed at mitigating oxidative stress and inflammation-related disorders.

Keywords: mulberry leaf protein; enzymatic hydrolysis; oxidative stress; anti-inflammatory; natural antioxidants

check for updates

Academic Editors: Raquel Bridi and Christian Espinosa-Bustos

Received: 20 May 2025
Revised: 20 June 2025
Accepted: 25 June 2025
Published: 28 June 2025

Citation: Zhou, Y.; Liu, T.; Zhang, R.; Wang, J.; Zhang, J.; Tong, Y.; Zhang, H.; Li, Z.; Si, D.; Wei, X. Bioactive Properties of Enzymatically Hydrolyzed Mulberry Leaf Proteins: Antioxidant and Anti-Inflammatory Effects. *Antioxidants* **2025**, *14*, 805. https://doi.org/10.3390/antiox14070805

Copyright: © 2025 by the authors. Licensee MDPI, Basel, Switzerland. This article is an open access article distributed under the terms and conditions of the Creative Commons Attribution (CC BY) license (https://creativecommons.org/licenses/by/4.0/).

1. Introduction

Oxidative stress is characterized by the excessive accumulation of reactive oxygen species (ROS) that induce cellular damage through oxidative modifications of DNA, proteins, and lipid biomolecules [1]. Although ROS are important signaling molecules in the immune system, excessive accumulation of ROS activates many oxidative stress signaling pathways and in turn exacerbates the inflammatory cascades [2–4]. Current evidence indicates that pattern recognition receptors, including Toll-like receptors (TLRs), RIG-I-like receptors (RLRs), and NOD-like receptors (NLRs), recognize pathogen-associated

molecular patterns (PAMPs) and damage-associated molecular patterns (DAMPs), which subsequently initiate mitochondrial- and NADPH oxidase-dependent ROS generation [5–8]. This redox signaling promotes the secretion of pro-inflammatory cytokines such as IL-1β and TNF-α/β, ultimately contributing to systemic tissue damage [9,10]. These findings collectively suggest a self-amplifying cycle between oxidative stress and inflammation in pathological processes [11].

Dietary antioxidant supplementation has emerged as a promising strategy for mitigating oxidative damage and improving health status [12,13]. In contrast, synthetic antioxidants like butylated hydroxyanisole (BHA) and butylated hydroxytoluene (BHT) have raised potential toxicity concerns [14,15]. Natural antioxidants are increasingly favored due to their superior safety and metabolic stability [16,17]. This paradigm shift highlights the importance of developing bioactive compounds from natural substrates. The antioxidant activity of proteins and peptides is fundamentally linked to their amphiphilic nature, which enables interactions with both hydrophilic radicals and hydrophobic cell membranes or oxidized lipids [18]. This dual solubility allows amphiphilic peptides to scavenge free radicals such as hydroxyl and peroxyl radicals at aqueous–lipid interfaces, chelate pro-oxidant metals, and disrupt lipid peroxidation chains [19]. Mulberry leaf (*Morus alba* L.), a traditional medicinal herb, has attracted considerable scientific interest as it contains a variety of bioactive substances including phenolic compounds, flavonoids, alkaloids, polysaccharides, and sterols [20,21]. Furthermore, it has been reported that mulberry leaf exhibits antioxidant and anti-inflammatory activities [22]. Mulberry leaf proteins exist predominantly as albumin, characterized by high β-sheet structures conferring exceptional thermal stability [23]. Their amphiphilic nature enables interactions with both hydrophilic radicals and hydrophobic membranes, facilitating antioxidant activities such as free radical scavenging and lipid peroxidation disruption [24]. Contemporary pharmacological studies have further validated the therapeutic potential of mulberry leaf proteins (MLP), particularly their antioxidant and medicinal properties [21,25–27].

However, the direct utilization of native MLP faces significant challenges. Native plant proteins often exhibit limited gastrointestinal absorption due to their high-molecular-weight tertiary structures and resistance to digestive enzymes [23]. Further, plant proteins may possess poor solubility, weak emulsifying capacity, and low thermal stability, restricting their application in functional foods or pharmaceuticals [28]. To overcome these limitations, enzymatic hydrolysis has become a critical strategy for converting native proteins into bioactive peptides. Proteases hydrolyze specific peptide bonds in proteins via cleavage site specificity, generating low-molecular-weight peptides [29]. These peptides exert bioactivities due to sequence-specific interactions with biological targets [30] Although, enzyme cleaving is sensitive to pH and inorganic salt, it has a lot of advantages such as specificity, safety, mild condition, and bioactive enhancement [31]. Thus, enzymatic hydrolysis has become the predominant methodology for bioactive peptide production, offering advantages in process safety, cost-effectiveness, and reaction controllability [32–34]. Previous investigations have demonstrated that protein hydrolysates from various sources, such as pepsin/trypsin-digested rapeseed protein and papain-hydrolyzed grass carp sarcoplasmic proteins, have significant antioxidant activity [35,36]. However, the antioxidant potential of MLP hydrolysates remains underexplored. Therefore, this study aims to optimize the parameters for the enzymatic hydrolysis of MLP into peptides, to systematically evaluate the anti-inflammatory and antioxidant activities of the hydrolysis products, and to elucidate the correlation between degree of hydrolysis (DH) and antioxidant activity.

2. Materials and Methods

2.1. Materials

Mulberry leaves (Guangdong Mulberry 69851) were purchased from the mulberry base of Long'an County, Guangxi Longhai Tianyuan Fruit and Vegetable Planting Family Farm. Mulberry leaves were air-dried, then oven-dried at 55 °C to constant weight. The dried leaves were pulverized in a crusher and sieved through a 60-mesh sieve to obtain mulberry leaf powder. MLP was isolated using the extraction procedures previously outlined by Chen et al. [37]. The powder was mixed with deionized water, and the pH was adjusted to 11.0. The mixture underwent ultrasonic treatment (235 W, 4.9 min) at 30 °C. After centrifugation (6000× *g*, 10 min), the supernatant was collected and adjusted to pH 4.0. Following 20 min incubation, the solution was re-centrifuged (8000× *g*, 10 min). The precipitate was washed twice with deionized water, redissolved, neutralized, and desalted for 48 h using a 3.5-kDa MWCO dialysis membrane. The extract rate was 34.12% and the desalted MLP extract was stored at −20 °C.

Penicillin–streptomycin mixture (100×), bovine serum albumin standard solution, BCA protein assay kit, SDS-PAGE gel preparation kit, papain (Pa), protamex (Pro), alkaline protease (Alk), trypsin (Try), and Coomassie Brilliant Blue G-250 were purchased from Beijing Solaibao Technology Co., Ltd. (Beijing, China). Neutral protease (Neu) was purchased from Aoboxing Biotechnology Co., Ltd. (Beijing, China). The CCK-8 assay kit was purchased from Beijing Lanjieke Technology Co., Ltd. (Beijing, China). N-1-naphthylethylenediamine hydrochloride and anhydrous p-aminobenzenesulfonic acid were purchased from Shanghai Macklin Biochemical Technology Co., Ltd. (Shanghai, China). ChamQ SYBR Color qPCR Master Mix (Without ROX) was purchased from Nanjing Vazyme Biotechnology Co., Ltd. (Nanjing, China). M5 Super qPCR RT kit with gDNA remover was purchased from Beijing Huagoumei Biotechnology Co., Ltd. (Beijing, China). IL-6 Elisa kit was purchased from Invitrogen Biotechnology Co., Ltd. (Shanghai, China). All reagents, unless otherwise specified, are of analytical reagent grade (AR).

2.2. Protease Activity and Enzymatic Hydrolysis of MLP

Protease activity was assayed following GB/T 23527-2009 [38]. Then, 0.2 mL of diluted enzyme was mixed with 0.2 mL of casein solution (20 g/L in 50 mM Tris-HCl, pH 7) and incubated at 70 °C for 10 min. The reaction was quenched with 0.4 mL of 65.4 g/L trichloroacetic acid (TCA). After vortexing and centrifugation (12,000× *g*, 4 °C, 5 min) (high-speed refrigerated centrifuge 5424R, Eppendorf AG, Hamburg, Germany), 0.4 mL of supernatant was mixed with 2 mL of 42.4 g/L Na_2CO_3 and 0.4 mL of Folin–Ciocalteu reagent (1 M). Following incubation at 40 °C for 20 min, absorbance was measured at 680 nm against a control (full-wavelength microplate reader SpectraMax M5E, Meigu Molecular Instruments, Inc., Rockville, MD, USA). A substrate-negative control was included. One unit (U/g) was defined as the enzyme amount, releasing 1 μg tyrosine per minute under assay conditions.

According to Monteiro et al. [39], MLP was dissolved in deionized water (1%, *w*/*v*) and heat in a water bath (DK-8A, Shanghai Precision Experimental Equipment Co., Ltd., Shanghai, China) at 90 °C to eliminate the interference of protease inhibitors in MLP. After cooling to room temperature, the mixture was hydrolyzed for 2 h under the conditions listed in Table 1. Then, the protease was inactivated by boiling in a water bath for 10 min. The mixture was centrifuged at 5000× *g* for 10 min, and the supernatant was collected. After dialysis (using deionized water) for 48 h using a dialysis bag with a molecular weight cutoff of 100 Da, the hydrolysate was freeze-dried to obtain the mulberry leaf protease hydrolysate, which was stored at −20 °C.

Table 1. Optimum enzymatic conditions and actual enzyme activities of five proteases.

Enzyme	Labeled Enzyme Activity (10^5 U/g)	Actual Enzyme Activity (10^5 U/g)	Optimum pH	Optimum Temperature (°C)	Enzyme Addition (U/g)
Alk	20	14.85	10	45	6000
Try	25	4.79	8	37	6000
Pa	8	6.78	7	55	6000
Pro	1	0.91	7	55	6000
Neu	6	8.52	7	45	6000

Notes: Alk, Try, Pa, Pro, and Neu represent alkaline protease, trypsin, papain, protamex, and neutral protease, respectively.

2.3. Degree of Hydrolysis

O-phthalaldehyde (OPA) was used to determine the DH according to the method of Nielsen et al. [40]. Samples were taken every 15 min. A volume of 0.2 mL of the sample was added to 1.5 mL of OPA reagent, mixed well, and left to stand for 2 min before immediately measuring the absorbance at 340 nm (OD340). The standard and blank groups used serine standard solution (0.9516 mM, 50 mg of serine was dissolved in 500 mL of deionized water) and deionized water, respectively. The DH was calculated using the following formula:

$$\text{Serine} - \text{NH}_2 = \frac{\text{OD}_\text{S} - \text{OD}_\text{B}}{\text{OD}_\text{St} - \text{OD}_\text{B}} \times 0.9516 \text{ meqv/L} \times \frac{0.1 \times 100}{\text{m}} \text{L/g protein} \quad (1)$$

$$\text{h} = \frac{\text{Serine} - \text{NH}_2 - \beta}{\alpha} \text{meqv/g protein} \quad (2)$$

$$\text{DH}(\%) = \frac{\text{h}_1 - \text{h}_0}{\text{h}_\text{tot}} \times 100 \quad (3)$$

where "Serine-NH_2" represents the millimolar number of amino groups contained in serine in the sample; "OD_S, OD_B, and OD_{St}" represent the OD_{340} values of the experimental group, blank group, and standard group, respectively; "α, β, and h_{tot}" are taken as 1.0, 0.4, and 8.166 mmol/g, respectively [41]; "m" represents the mass of protein in the mulberry leaf protease hydrolysis product; "h_0 and h_1" represent the degree of hydrolysis relative to the original substrate before and after the hydrolysis reaction.

2.4. TCA-Soluble Peptide

Then, 3 mL of the sample was uniformly mixed with 3 mL of 10% (*w*/*v*) TCA solution. After standing for 0.5 h, the mixture was centrifuged at 5000× *g* for 10 min and the supernatant was collected. The protein concentration of the sample was determined before and after mixing using the Lowry method [42], and the values were recorded as T_B and T_A, respectively. The yield of TCA-soluble peptide can be calculated using the following formula:

$$\text{Yield of TCA} - \text{soluble piptide } (\%) = \frac{\text{T}_\text{A}}{\text{T}_\text{B}} \times 100 \quad (4)$$

where "T_A, T_B" represent the protein concentration of the sample before and after mixing.

2.5. Molecular Weight Distribution of Hydrolysate

Then, 160 µL of the sample (1.2 mg/mL) was mixed with 40 µL of loading buffer, and then the proteins were denatured by heating in a water bath at 100 °C for 10 min. After cooling to room temperature, the mixture was loaded into the wells of the protein gel. The method for preparing the protein gel is referred to in Table 2. The electrophoresis program was set to run at 80 V for 30 min, followed by 120 V for 60 min.

Table 2. Protein gel configuration method.

Concentration of Gel	15%	5%
Volume	10 mL	5 mL
30%Acr/Bis (29:1)	5 mL	830 μL
1.5 M Tris-HCl (pH = 8.8)	2.5 mL	0
1.0 M Tris-HCl (pH = 6.8)	0	625 μL
10%SDS	100 μL	50 μL
10%APs	100 μL	75 μL
TEMED	10 μL	7.5 μL
H_2O	2.3 mL	3.42 mL

The molecular weight distribution was determined using a Waters 2695 high-performance liquid chromatography (HPLC) system equipped with a 2487 UV detector and workstation GPC software empower 3 (Waters Inc., Milford, MA, USA). A sample of 100 mg was dissolved in 10 mL of mobile phase (acetonitrile/water/trifluoroacetic acid, 40/60/0.1, *v*/*v*/*v*). After ultrasonication for 5 min, the solution was filtered through a 0.22 μm membrane filter, and 10 μL of the filtrate was injected into the HPLC system. The chromatographic column used was a TSKgel 2000 SWXL (300 mm × 7.8 mm), with a flow rate of 0.5 mL/min, column temperature of 30 °C, and detection wavelength of 220 nm. Cytoglobin (MW 12,384 Da), aprotinin (MW 6500 Da), bacitracin (MW 1422 Da), glycyl-glycyl-tyrosyl-arginine (MW 451 Da), and glycyl-glycyl-glycine (MW 189 Da) were used as standards for the molecular weight calibration curve.

2.6. Antioxidant Activity

2.6.1. Reducing Power

The reducing power was tested according to Agnieszka et al. [43], where 1 mL sample (1 mg/mL) was mixed with 2.5 mL sodium carbonate buffer (0.2 M, pH 6.6) and 2.5 mL 1% (*w*/*v*) potassium ferricyanide, shaken vigorously, and incubated at 50 °C for 20 min. Then, 2.5 mL 10% (*w*/*v*) trichloroacetic acid (TCA) was added, and the mixture was centrifuged at 867× *g* for 10 min. The supernatant (2.5 mL) was combined with 2.5 mL deionized H_2O and 0.5 mL 0.1% (*w*/*v*) $FeCl_3$, left at RT for 10 min, and absorbance measured at 700 nm (OD_{700}). Vitamin C (same conc. as sample) was the positive control.

2.6.2. ABTS Radical Scavenging Activity

The referred method was from Chaturved et al. [44], with minor optimization, where 7 mM ABTS and 2.4 mM potassium persulfate solution (1:1) was incubated in the dark at RT for 16 h to form ABTS. This was diluted with PBS (pH 7.4) to OD_{734} = 0.70 ± 0.02. Then, 300 μL sample (0.1 mL/mL) was added to 2 mL ABTS working solution, incubated in the dark at RT for 10 min, and absorbance measured at 734 nm (A_1). Vitamin C served as the positive control. The ABTS radical scavenging rate is calculated using the following formula:

$$\text{ABTS free radical scavenging ratio } (\%) = \left(1 - \frac{A_1 - A_0}{A}\right) \times 100 \quad (5)$$

where A_0 represents OD_{734} obtained by replacing ABTS with deionized water; A represents OD_{734} obtained by replacing sample with ionized water.

2.6.3. OH Free Radical Scavenging Ratio

OH radical scavenging ratio was determined according to the method of Luo et al. [45], by adding 1.5 mL of salicylic acid (1.8 mM), 2 mL of ferrous sulfate (1.8 mM), and 1 mL of

hydrogen peroxide (6 mM) successively to 1 mL of the sample (0.1 mL/mL). After thorough mixing by shaking, the mixture was allowed to react at 37 °C for 30 min. Then it was centrifuged at 3000 r/min for 5 min. The absorbance of the supernatant was measured at 510 nm (OD_{510}) as A_1.

$$\text{OH free redical scavenging ratio } (\%) = \left(1 - \frac{A_1 - A_0}{A}\right) \times 100 \quad (6)$$

where A_0 represents OD_{510} obtained by replacing salicylic acid with deionized water; A represents OD_{510} obtained by replacing sample with deionized water.

2.6.4. DPPH Free Radical Scavenging Ratio

The procedure and methods of testing antioxidant activity referred to Zhou et al. [46], by adding 1 mL of the sample (0.1 mL/mL) to 2 mL of the DPPH working solution. After thorough mixing by shaking, the mixture was allowed to react in the dark at room temperature for 30 min. The absorbance was measured at 517 nm (OD_{517}) as A_1. Vitamin C was used at the same concentration as the sample and the positive control. The DPPH radical scavenging rate was calculated using the following formula:

$$\text{DPPH free redical scavenging ratio } (\%) = \left(1 - \frac{A_1 - A_0}{A}\right) \times 100 \quad (7)$$

where A_0 represents OD_{517} obtained by replacing DPPH with ethanol; A represents OD_{517} obtained by replacing sample with deionized water.

2.7. Cytotoxicity

According to the results of DH and test of antioxidant activity, NeuH showed good antioxidant capacity, so it was selected for the next step of the experiment. IPEC-J2 cells, HepG2 cells, and RAW 264.7 cells were diluted with complete culture medium (90% DMEM + 10% fetal bovine serum (FBS) + 1% penicillin–streptomycin (PS)) and then seeded into a 96-well plate and cultured for 24 h. For the experimental group, 100 µL NeuH samples diluted to different concentrations using DMEM were added into cells. For the control group, 100 µL DMEM was added into cells. For the blank group, only 100 µL DEME was added to the wells (without cells). After 24 h of cell culture, CCK-8 working solution (90% DMEM + 10% CCK-8) was added to each well. The plates were incubated until the OD_{450} of the blank group reached around 1.0. The cell viability was calculated using the following formula:

$$\text{Survival rate of cell } (\%) = \frac{OD_S - OD_B}{OD_C - OD_B} \times 100 \quad (8)$$

where OD_S, OD_B, and OD_C represent OD450 obtained as experimental group, blank group, and control group.

2.8. Anti-Inflammatory Activity

2.8.1. Nitric Oxide (NO) Analysis

RAW 264.7 cells (5×10^4 cells/mL) in complete medium (90% DMEM, 10% FBS, 1% P/S) were seeded (100 µL/well) in a 96-well plate and incubated overnight. Experimental wells received 100 µL serum-free DMEM with NeuH (100–800 µg/mL); blank and model groups received serum-free DMEM. After 6 h, LPS (100 ng/mL final conc.) was added to model and experimental groups, while blank received DMEM. After 24 h, supernatant NO levels were quantified via Griess reagent [47].

2.8.2. Gene Transcription Level

RNA was extracted using Trizol (Beyotime Biotech, Shanghai, China), integrity checked by agarose gel electrophoresis, and conc. measured by microvolume spectrophotometry. RNA was reverse-transcribed to cDNA with the M5 Super qPCR RT kit (Mei5bio Biotech, Beijing, China). RT-PCR used ChamQ SYBR Color qPCR Master Mix (Vazyme Biotech, Nanjing, China) on a LightCycler® 96 (Roche, Risch-Rotkreuz, Switzerland) to quantify inflammation-related gene expression (Table 3). Primers for GAPDH, COX-2, IL-6, and iNOS (Sangon Biotech, Shanghai, China) are listed in Table 4. qPCR conditions: 95 °C, 30 s; 40 cycles of 95 °C, 10 s and 60 °C, 10 s; melting curve: 95 °C, 5 s; 60 °C, 60 s; 95 °C, 1 s. mRNA levels were analyzed.

Table 3. RT-PCR reaction system.

Component	Volume
2 × ChamQ SYBR Color qPCR Master Mix (without ROX)	10.0 μL
Upstream primer (10 μM)	0.4 μL
Downstream primer (10 μM)	0.4 μL
cDNA template	1.0 μL
ddH_2O	8.2 μL

Table 4. RT-PCR primer sequence list.

Gene	Gene Accession Number	Sequence
GAPDH	AC166162	F: 5′-TGAAGGTCGGAGTCAACGG-3′ R: 5′-TCCTGGAAGATGGTGATGGG-3′
COX-2	DQ874614	F: 5′-CTGCAAGTGCATCATCGTTGTTC-3′ R: 5′-CTGCAAGTGCATCATCGTTGTTC-3′
IL-6	AC112933	F: 5′-TACCACTTCACAAGTCGGAGGC-3′ R: 5′-CTGCAAGTGCATCATCGTTGTTC-3′
iNOS	AF427516	F: 5′-GAGACAGGGAAGTCTGAAGCAC-3′ R: 5′-CCAGCAGTAGTTGCTCCTCTTC-3′

2.8.3. Cytokine Analysis

After 24 h of LPS treatment, the cell culture supernatant was collected. The concentration of the inflammatory cytokine IL-6 in the supernatant was measured using an ELISA kit (Sigma-Aldrich, St. Louis, MO, USA).

2.9. Statistical Analysis

Each group of experiments was independently repeated three times, and the results were expressed as mean ± standard deviation. Excel 2019 and SPSS Statistics 27.0 were used for data processing and analysis. Graphpad prism 9.4.1 and Origin 2019 were used for diagram. One-way ANOVA was used for data analysis. $p \leq 0.05$ was considered significant.

3. Results

3.1. Hydrolysis of MLP and Production of Peptides

As shown in Figure 1A, the hydrolysis of MLP by different proteases varied greatly. The DH values of the five enzymes increased rapidly as the reaction progressed from 0 to 30 min. After 30 min, the rate of DH rise gradually slowed down for all these enzymes. TryH and PaH showed a similar tendency and reached their maximum DH around 90 min. The other hydrolysates reached their maximum DH at around 120 min. Figure 1B shows that NeuH had the highest DH value of 26.85 ± 1.17%, which was significantly higher than AlkH and ProH ($p < 0.05$), and significantly higher than TryH and PaH ($p < 0.01$). As shown

in Figure 1C, the highest TCA-soluble peptide yield of 39.98 ± 3.82% was obtained from the neutral protease digest of MLP followed by AlkH and ProH, and the lowest yields of 6.55 ± 0.53% and 3.66 ± 1.37% were obtained for TryH and PaH, respectively.

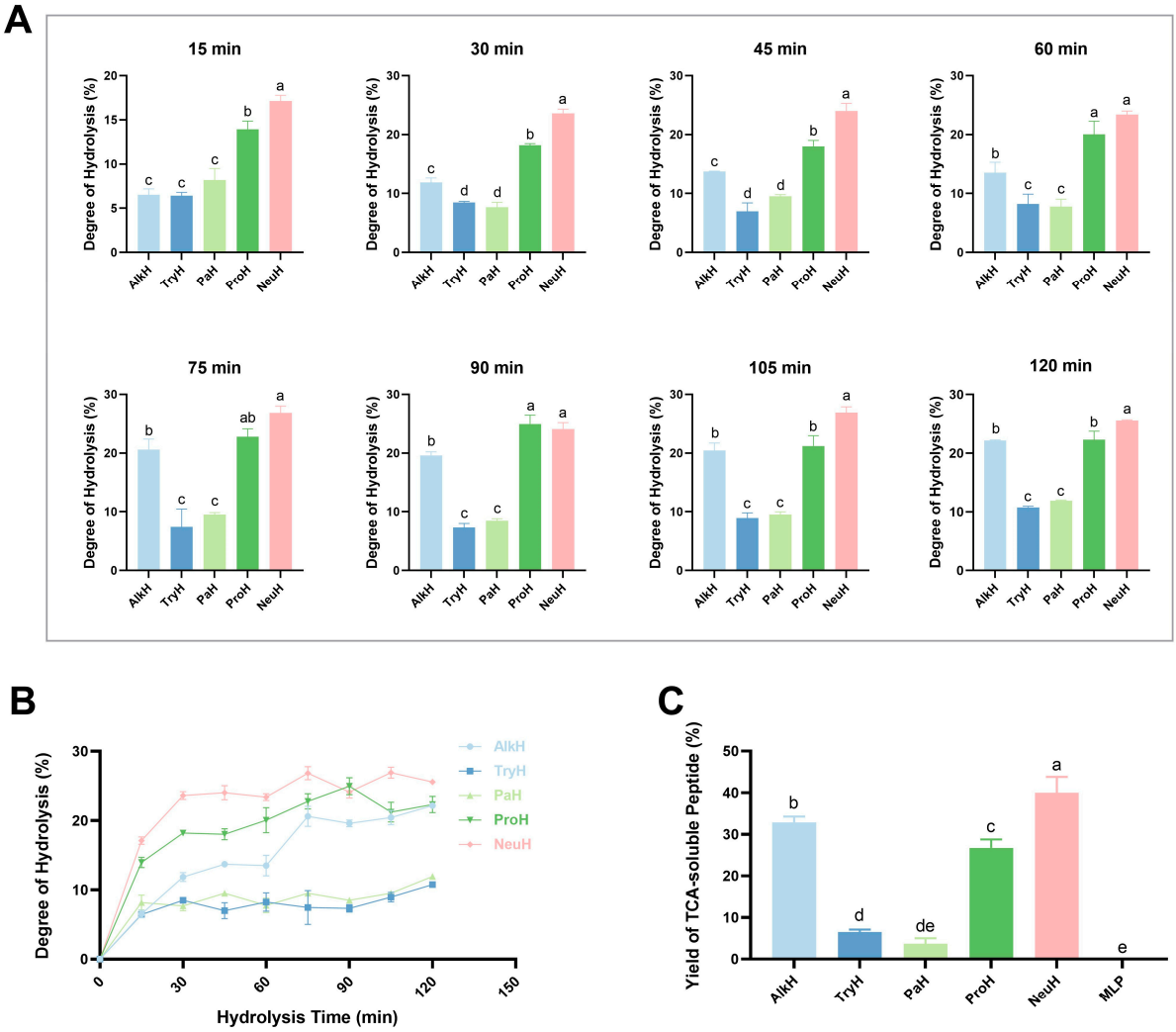


Figure 1. Degree of hydrolysis of mulberry leaf protein (MLP). (**A**) Degree of hydrolysis of MLP over time under different protease hydrolysis conditions; (**B**) hydrolysis degree curve within 2 h; (**C**) yields of TCA-soluble peptide ratio of MLP hydrolysate. Notes: AlkH, TryH, PaH, ProH, and NeuH represent alkaline protease, trypsin hydrolysate, papain hydrolysate, protamex hydrolysate, and neutral protease hydrolysate, respectively; different lowercase letters (a–e) indicate statistically significant differences between hydrolysates ($p \leq 0.05$); same lowercase letters indicate no statistically significant differences ($p > 0.05$).

3.2. SDS-PAGE and Molecular Weight Distribution

The SDS-PAGE electrophoresis results of MLP and its enzymatic hydrolysates are shown in Figure 2A. Enzymatic hydrolysis resulted in an increase in protein components smaller than 31 kDa in the five enzymatic hydrolysates, particularly for AlkH, ProH, and NeuH. Correspondingly, there was a noticeable decrease in the protein components distributed between 50 and 240 kDa in the hydrolysates of these three enzymes compared with the pre-hydrolysis period. The calibration curve for molecular weight (MW) distribution is depicted in Figure 2B,C.

The high-performance gel permeation chromatograms of MLP and its enzymatic hydrolysates are shown in Figure 2D–I, and the molecular weight distribution is presented in Table 5. The results indicate that the protein components with MW greater than 10 kDa

in MLP accounted for 56.24% of the total proteins. This was followed by TryH, PaH, AlkH, ProH, and NeuH. The protein components with molecular weights less than 1 kDa were most abundant in NeuH, reaching 41.50%. In the other four enzymatic hydrolysates, the proportion of protein components with molecular weights less than 3 kDa was significantly higher than that of MLP. DH of the five protease hydrolysates, from highest to lowest, was NeuH, ProH, PaH, AlkH, and TryH.

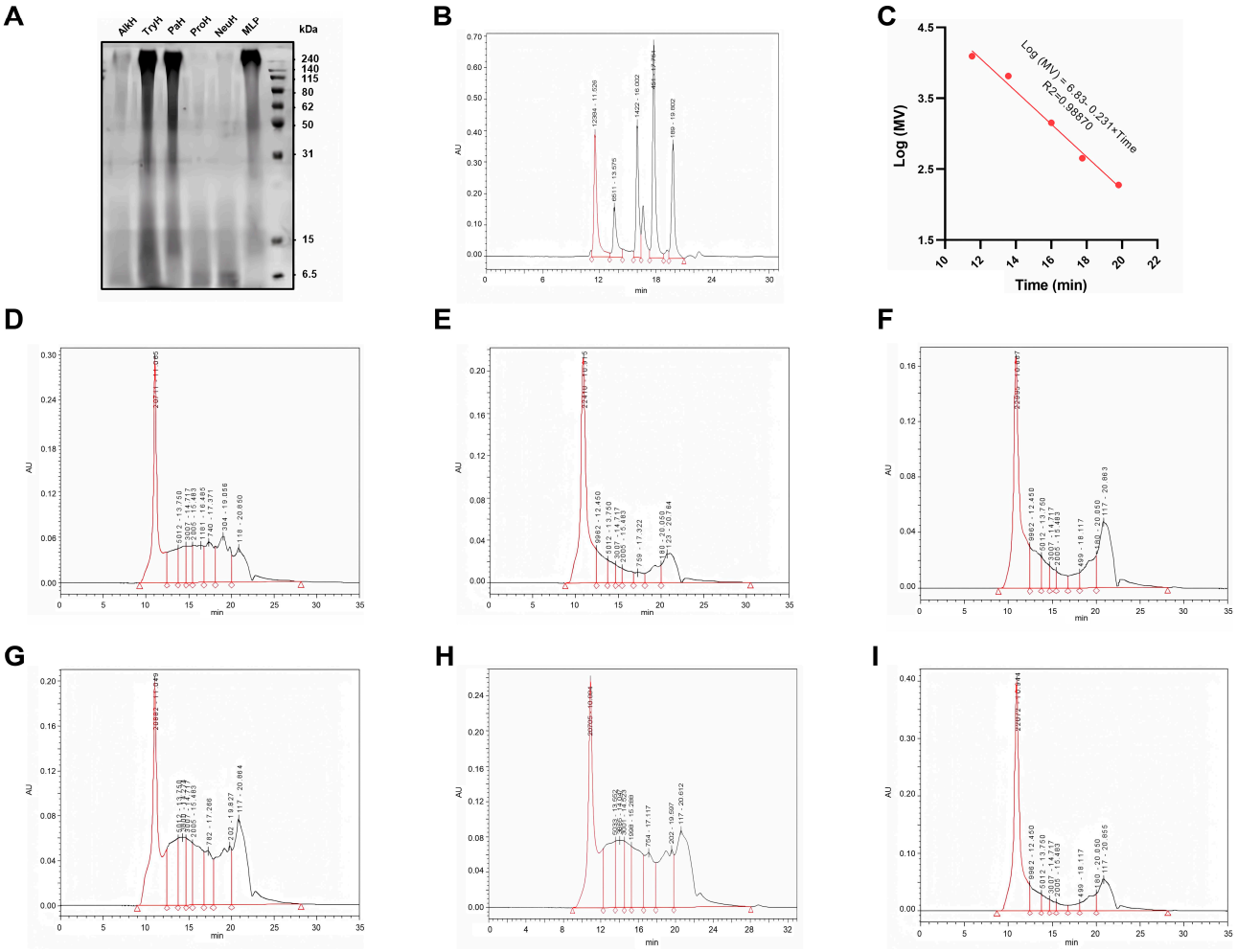


Figure 2. Molecular weight distribution of different hydrolysates. (**A**) SDS−PAGE electrophoresis of MLP and its hydrolysate; (**B**,**C**) scale curve for the determination of molecular weight distribution; (**D**–**I**) high performance gel permeation chromatogram of MLP, AlkH, TryH, PaH, ProH, and NeuH. Notes: AlkH, TryH, PaH, ProH, and NeuH represent alkaline protease, trypsin hydrolysate, papain hydrolysate, protamex hydrolysate, and neutral protease hydrolysate, respectively; MW means molecular weight; the "number-number" in (**B**,**D**–**I**) means "molecular weight (Da)-retention time (min)".

Table 5. Molecular weight distribution of MLP hydrolysate.

Sample	>10 kDa (%)	5–10 kDa (%)	3–5 kDa (%)	1–3 kDa (%)	<1 kDa (%)
MLP	56.24	7.83	3.92	4.68	27.43
AlkH	29.21	8.58	7.05	16.76	29.70
TryH	52.16	9.26	5.12	7.31	26.16
PaH	42.07	9.37	5.04	6.49	37.03
ProH	25.05	10.19	8.13	15.65	40.97
NeuH	23.66	10.71	8.31	15.92	41.50

Notes: AlkH, TryH, PaH, ProH, and NeuH represent alkaline protease, trypsin hydrolysate, papain hydrolysate, protamex hydrolysate, and neutral protease hydrolysate, respectively.

3.3. In Vitro Antioxidant Ability of MLP Hydrolysates

As shown in Figure 3A, NeuH and ProH had a greater reducing ability than MLP ($p < 0.05$), with 0.411 ± 0.002 and 0.392 ± 0.004, respectively. The OD_{700} values of the AlkH and MLP groups were similar ($p > 0.05$). However, PaH and TryH were significantly less antioxidant than MLP ($p < 0.05$). ABTS, OH, and DPPH free radical scavenging ratio of NeuH and AlkH were significantly higher than MLP ($p < 0.05$). For ABTS free radical (Figure 3B), ProH had a stronger antioxidant ability compared with MLP ($p < 0.05$), whereas PaH and TryH had a poorer antioxidant activity ($p > 0.05$). In the test of OH free radical scavenging ratio (Figure 3C), PaH and ProH had no significant differences compared with MLP ($p > 0.05$), but TryH group was significantly lower ($p < 0.05$). According to Figure 3D, all hydrolysates had a higher scavenging activity for DPPH free radicals than MLP ($p < 0.05$), except TryH, which had a similar scavenging activity as MLP ($p > 0.05$). Considering that NeuH is more capable in various aspects, NeuH was chosen to conduct further investigation. In addition, as shown in Table 6, the antioxidant activity of the enzymatic hydrolysis products of MLP was significantly ($p < 0.01$) correlated with the yield and degree of hydrolysis of TCA soluble peptides ($p < 0.01$).

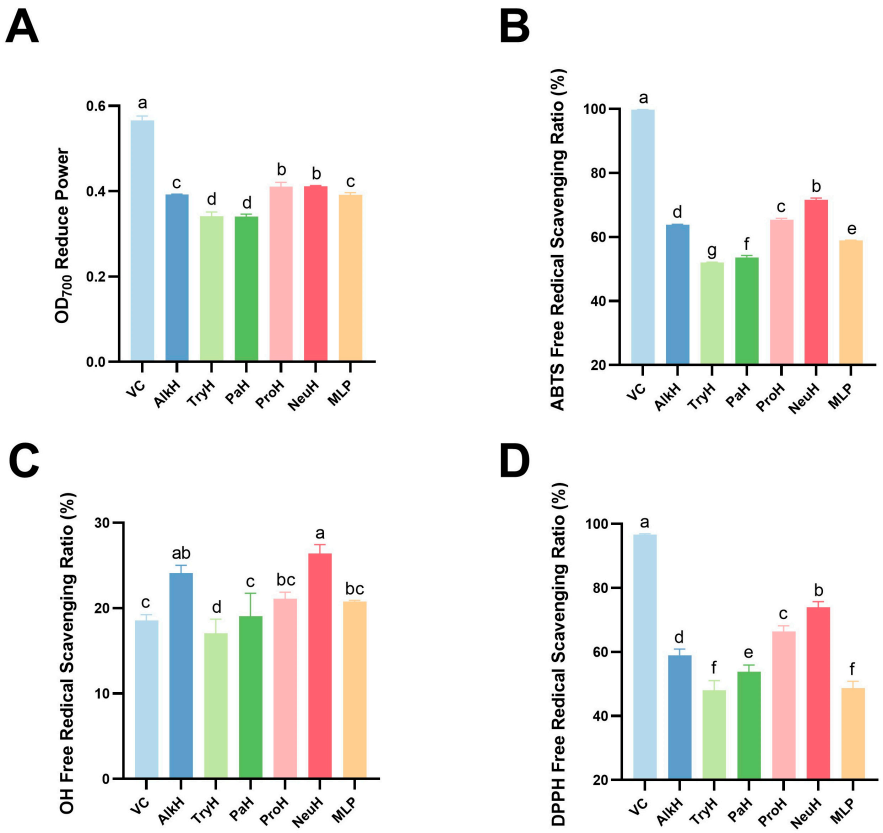


Figure 3. Antioxidant activity of different hydrolysates. (**A**) OD700 reduced power of different hydrolysates; (**B**) ABTS free radical scavenging ratio of different hydrolysates; (**C**) OH free radical scavenging ratio of different hydrolysates; (**D**) DPPH free radical scavenging ratio of different hydrolysates. Notes: VC, AlkH, TryH, PaH, ProH, and NeuH represent vitamin C alkaline protease, trypsin hydrolysate, papain hydrolysate, protamex hydrolysate, and neutral protease hydrolysate, respectively; different lowercase letters (a–g) indicate statistically significant differences between hydrolysates ($p \leq 0.05$); same lowercase letters indicate no statistically significant differences ($p > 0.05$).

Table 6. Correlation analysis of the antioxidant activity of MLP hydrolysate with hydrolysis-related indexes.

Items	YTP	DH	RP	DPPH	ABTS	OH
YTP	1.000	0.931 **	0.917 **	0.873 **	0.868 **	0.959 **
DH	0.931 **	1.000	0.949 **	0.853 **	0.908 **	0.978 **
RP	0.917 **	0.949 **	1.000	0.000	0.920 **	0.983 **
DPPH	0.873 **	0.853 **	0.000	1.000	0.141	0.064
ABTS	0.868 **	0.908 **	0.920 **	0.141	1.000	0.964 **
OH	0.959 **	0.978 **	0.983 **	0.064	0.964 **	1.000

Notes: "YTP" represents "yield of TCA-soluble peptide"; "DH" represents "degree of hydrolysis"; "RP" represents reducing power"; "DPPH" represents "scavenging rates of DPPH"; "ABTS" represents "scavenging rates of ABTS"; "OH" represents "scavenging rates of OH"; "**" indicates highly significant differences ($p < 0.01$).

3.4. Cell Cytotoxicity of NeuH

As shown in Figure 4A, the survival rate of IPEC-J2 cells decreased with increasing concentrations of NeuH. The survival rate of IPEC-J2 cells was 87.01 ± 3.41% at 600 μg/mL NeuH concentration. As the concentration of NeuH increased, HepG2 cell viability initially decreased and then increased (Figure 4B). The lowest survival rate of 93.69 ± 2.56% was observed at a concentration of 100 μg/mL. The cell survival rate was 106 ± 2.64% at a concentration of 800 μg/mL, which was significantly higher than that of the control group ($p < 0.05$). As demonstrated in Figure 4C, the survival rate of RAW 264.7 cells was significantly higher than that of the control group in the concentration range of 100 to 800 μg/mL ($p < 0.05$).

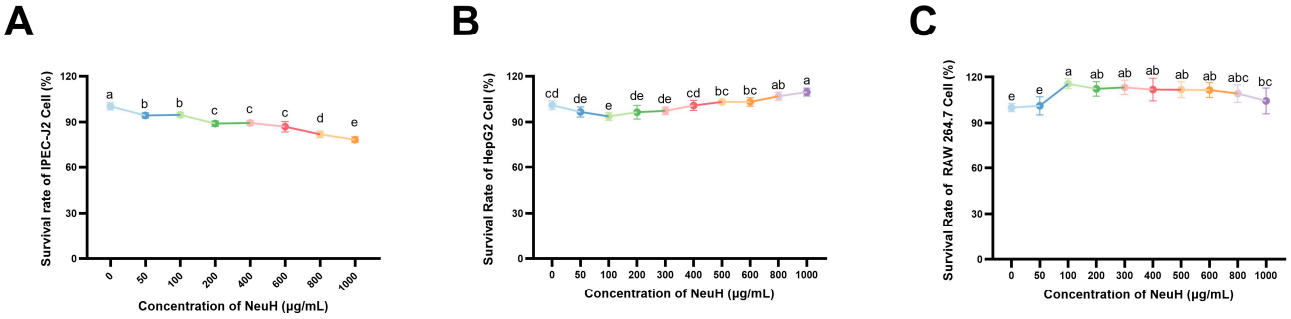


Figure 4. Effects of different concentration of NeuH on cell ($n = 6$). (**A**) Survival rate of IPEC-J2 cell; (**B**) survival rate of HepG2 cell; (**C**) survival rate of RAW264.7 cell. Notes: NeuH represents neutral protease hydrolysate; different lowercase letters (a–e) indicate statistically significant differences between different concentrations ($p \leq 0.05$); same lowercase letters indicate no statistically significant differences ($p > 0.05$).

3.5. Effect of NeuH on LPS-Induced Inflammation in RAW 264.7 Cell

Nitric oxide (NO) secretion was significantly higher in the LPS group than in the blank control group ($p < 0.01$), indicating that the inflammatory model was successfully established (Figure 5A). NeuH significantly reduced NO secretion of RAW 264.7 cells ($p < 0.01$), and a concentration-dependent trend was observed within the concentration range of 100–600 μg/mL. The effect of NeuH on the secretion of IL-6 cytokine by RAW 264.7 cells is depicted in Figure 5B. NeuH significantly reduced LPS-induced secretion of the inflammatory cytokine IL-6 ($p < 0.01$) in a concentration-dependent manner. LPS stimulation for 24 h significantly upregulated gene transcription of IL-6 (Figure 5C), iNOS (Figure 5D) and COX-2 (Figure 5E). Treatment with NeuH significantly downregulated the transcription of IL-6, iNOS, and COX-2 genes ($p < 0.001$) (Figure 5C–E).

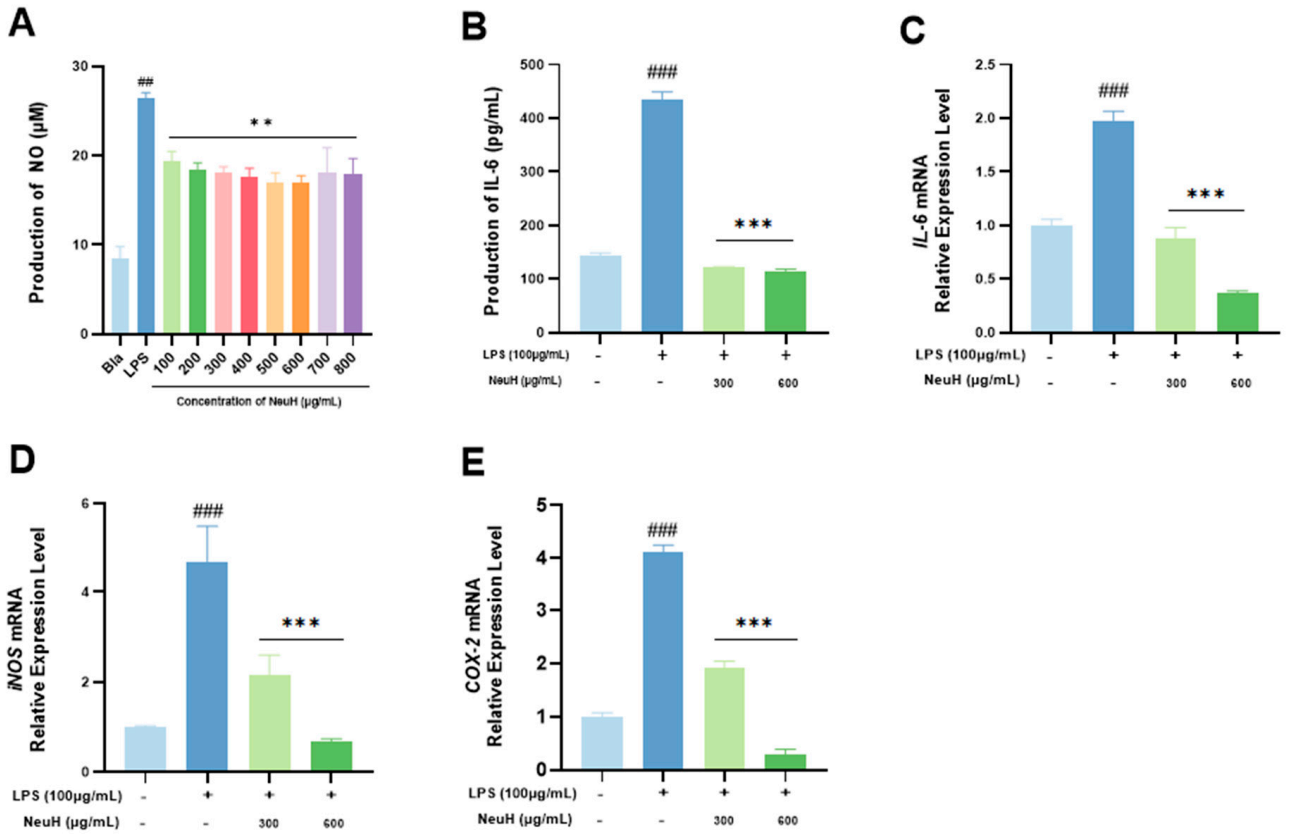


Figure 5. Effect on inflammation in RAW 264.7 cell of NeuH (n = 6). (**A**) Effect on NO production with NeuH in different concentration; (**B**) effect on IL-6 production with NeuH in different concentration. (**C**) Effect on IL-6 gene transcription with NeuH in different concentration; (**D**) effect on iNOS gene transcription with NeuH in different concentration; (**E**) effect on COX-2 gene transcription with NeuH in different concentration. Notes: Bla represents blank group; NeuH represents neutral protease hydrolysate; "##" means the difference is significantly compared with control group ($p < 0.01$), "###" means the difference is significantly compared with control group ($p < 0.001$), "**" means the difference is significantly compared with LPS group ($p < 0.01$), "***" means the difference is significantly compared with LPS group ($p < 0.001$).

4. Discussion

In recent years, oxidative stress and its associated pathologies have emerged as an active area of research [48–50]. The accumulation of oxidative stress contributes to the development of uremia and various vascular disorders [51–53]. Research has demonstrated that dietary supplementation with specific natural antioxidants can aid in the prevention of these conditions [54–57]. Consequently, the investigation of antioxidants is crucial for advancing human health. Numerous studies have reported that MLP enhances immune function through its antioxidant properties [58–60]. Studies indicate that protein hydrolysates exert beneficial health effects, including antioxidant, antihypertensive, and anticancer activities [61,62]. Therefore, in this study, we hydrolyzed MLP using five common proteases to enhance its bioactive properties.

Among the five enzymes tested, Neu exhibited the highest degree of hydrolysis (DH) for MLP, indicating significant variation in enzymatic efficacy toward the same substrate. This observation aligns with Bavaro et al. [63], who reported Neu's superior activity and regioselectivity across diverse substrates—likely explaining its optimal catalytic efficiency in our study. Trichloroacetic acid (TCA) selectively denatures and precipitates high-molecular-weight proteins while exerting minimal effects on low-molecular-weight proteins and peptides [64–66]. Consistent with Neu's high DH, NeuH yielded the highest TCA-soluble

peptide content among the hydrolysates. Similar substrate-specific efficiency was documented for wheat germ (*Triticum vulgare*) globulin hydrolysis [67]. Given Neu's status as the most prominent and extensively utilized enzyme [68], these findings hold broad relevance. Electrophoretic analysis revealed residual 50–240 kDa protein components in TryH and PaH, despite increased 6.5–15 kDa protein/peptide content. In contrast, AlkH, ProH, and NeuH showed near-complete hydrolysis of high-molecular-weight proteins into smaller fragments. Notably, substantial evidence confirms that low-molecular-weight proteins and peptides (<15 kDa) exhibit potent antioxidant and anti-inflammatory activities [69–71]. This strongly suggests that enzymatic hydrolysis potentiates MLP's biofunctional properties through generation of bioactive peptides.

Previous studies have demonstrated that MLP possesses notable antioxidant properties [58,72]. This experiment further investigated the hydrolysis of MLP with proteases in vitro and found that the antioxidant activity of the hydrolyzed products surpassed that of MLP itself. Compared with MLP, hydrolysis with neutral protease at a concentration of 0.1 mg/mL increased the scavenging rates of ABTS, DPPH, and OH free radicals by 20.15%, 51.82%, and 26.90%, respectively, as well as the OD_{700} reducing power by 5.00%. Previous studies have indicated that the antioxidant properties of protein hydrolysates are closely related to their DH, with optimal hydrolysis conditions enhancing antioxidant activities [73,74]. However, not all studies align with this, e.g., excessive hydrolysis can disrupt the structure of active peptides, resulting in reduced activity [31,75]. Therefore, the relationship between DH and antioxidant activity is complex and may depend on the exposure sites of the active groups within the hydrolysates. As for hydrolysates of MLP, our results show that, with the higher DH, the bioactive peptides exhibited superior antioxidant capability, suggesting a potential positive correlation between DH and antioxidant activity.

Cell viability is a fundamental indicator of cell growth and can be used to evaluate the impact of culture conditions and the environment on cellular health [76,77]. In this study, HepG2, IPEC-J2, and RAW 264.7 cells, commonly used in antioxidant research, were selected for testing [78–80]. We found that, at a concentration of 100 μg/mL, HepG2 cell activity significantly decreased but, as the concentration of NeuH increased, cell activity gradually improved, even showing clear promotion of growth. The effect of NeuH on HepG2 cell viability was concentration-dependent, with a trend of increasing followed by decreasing activity, consistent with previous studies on the effect of renalase-derived peptides on HepG2 cell viability [81]. Surprisingly, the cells maintained good activity even with NeuH concentrations as high as 1000 μg/mL. Interestingly, IPEC-J2 cell viability decreased with increasing NeuH concentration, a result that appears inconsistent with similar studies [82]. A possible explanation is that IPEC-J2 cells may be highly sensitive to NeuH, leading to slight toxicity. For cell viability, 80–100% is generally considered to be non-toxic, 60–80% to be slightly toxic, and 40–60% to be moderately toxic [83–85]. In this experiment, the cell viability of IPEC-J2 at a NeuH concentration of 600 μg/mL was 87.01 ± 3.41%, indicating that NeuH is safe within the 0–600 μg/mL concentration range. Therefore, the effects of NeuH vary significantly between different cell types, with overall results suggesting that NeuH does not exhibit significant cytotoxicity and, to some extent, promotes cell growth.

Reactive oxygen species (ROS) not only induce oxidative stress but also mediate inflammation through the Toll-like receptor 4 (TLR4)/NF-κB signaling pathway [86,87]. ROS promote inflammatory cytokine secretion, activate downstream oxidant-producing enzymes, and generate additional ROS, thereby perpetuating a detrimental feedback loop that damages cells [88,89]. Antioxidant intervention can inhibit this cyclical progression [90–92]. In this study, we demonstrated that NeuH exhibits potent antioxidant activity. Consequently, we evaluated its potential anti-inflammatory effects using an LPS-induced RAW

264.7 cell inflammation model. LPS activates the NF-κB signaling pathway, leading to the upregulation of TNF-α, IFN-γ, IL-1β, IL-6, cyclooxygenase-2 (COX-2), and inducible nitric oxide synthase (iNOS) [93]. Consistent with previous reports [94,95], LPS stimulation significantly elevated the transcription levels of IL-6, COX-2, and iNOS genes, as well as IL-6 cytokine expression. Furthermore, LPS acts as an inflammatory inducer by stimulating macrophages to produce ROS via the TLR4 receptor [96]. Both the TLR4 receptor and its coreceptor MD2 are essential for macrophage recognition of LPS and play a pivotal role in LPS-induced inflammation [97]. NeuH treatment significantly suppressed these responses and reduced the expression of multiple inflammatory genes and cytokines. These findings suggest that NeuH exerts anti-inflammatory effects, at least partially, through inhibition of the TLR4/NF-κB signaling pathway. This mechanistic interpretation aligns with studies reporting that mung bean protein hydrolysate mitigates LPS-driven inflammatory cascades in macrophages via blockade of NF-κB nuclear translocation [98]. Similar anti-inflammatory activity has also been documented for soybean protein hydrolysates [99], thereby strengthening the foundational support for this study's key conclusions.

In summary, we selected the optimal enzyme for degrading MLP from a group of common proteases and conducted a preliminary analysis of the relationship between DH and antioxidant activity. While our results suggest a correlation between these two factors, further research is needed to confirm and generalize these findings. Furthermore, this study did not conduct animal experiments to verify the efficacy in vivo. Overall, the results provide a theoretical basis for the development of NeuH as a food additive or medicine with both antioxidant and anti-inflammatory properties.

5. Conclusions

In this study, we found that in vitro enzymatic hydrolysis of MLP could enhance its antioxidant activity. The hydrolysates obtained from neutral protease exhibited the highest antioxidant and anti-inflammatory activities. Furthermore, these hydrolysates showed no significant cytotoxicity. MLP showed better antioxidant activity with higher DH, suggesting that there might be a potential correlation between the above two indexes. These findings provide theoretical and technical support for the utilization of mulberry leaf resources and the development of MLP as novel natural antioxidant and anti-inflammatory agents.

Author Contributions: Conceptualization, Y.Z., J.W., and R.Z.; methodology, Y.Z., J.W., J.Z., and Y.T.; formal analysis, T.L., Y.Z., J.W., Z.L., H.Z., and J.Z.; funding acquisition, R.Z., D.S., and X.W.; supervision, R.Z., D.S., and X.W.; writing—original draft, Y.Z., J.Z., Z.L., and H.Z.; writing—review and editing, Y.Z., T.L., R.Z., and X.W. All authors have read and agreed to the published version of the manuscript.

Funding: This research was funded by the National Key Research and Development Program of China (grant number 2022YFD1300900 and 2024YFD1300400), the National Natural Science Foundation of China (No. 32402776), Xinjiang Uygur Autonomous Region "Tianshan Talents" Cultivation Program (2024TSYCTD0016), China Agricultural University Young Talent Cultivation Program, and Xinjiang Uygur Autonomous Region "Tianchi Talent" Introduction Program.

Institutional Review Board Statement: Not applicable.

Informed Consent Statement: Not applicable.

Data Availability Statement: Data will be made available on request.

Conflicts of Interest: The authors declare no conflicts of interest.

References

1. Cross, C.E.; Halliwell, B.; Borish, E.T.; Pryor, W.A.; Ames, B.N.; Saul, R.L.; Mccord, J.M.; Harman, D. Oxygen Radicals and human-disease. *Ann. Intern. Med.* **1987**, *107*, 526–545. [CrossRef]
2. West, A.P.; Shadel, G.S.; Ghosh, S. Mitochondria in innate immune responses. *Nat. Rev. Immunol.* **2011**, *11*, 389–402. [CrossRef]
3. Kaminski, M.M.; Roth, D.; Krammer, P.H.; Gulow, K. Mitochondria as oxidative signaling organelles in T-cell activation: Physiological role and pathological implications. *Arch. Immunol. Ther. Exp.* **2013**, *61*, 367–384. [CrossRef] [PubMed]
4. Mittal, M.; Siddiqui, M.R.; Tran, K.; Reddy, S.P.; Malik, A.B. Reactive oxygen species in inflammation and tissue injury. *Antioxid. Redox Signal.* **2014**, *20*, 1126–1167. [CrossRef] [PubMed]
5. Chen, G.Y.; Nunez, G. Sterile inflammation: Sensing and reacting to damage. *Nat. Rev. Immunol.* **2010**, *10*, 826–837. [CrossRef] [PubMed]
6. Iwasaki, A.; Medzhitov, R. Regulation of adaptive immunity by the innate immune system. *Science* **2010**, *327*, 291–295. [CrossRef]
7. Takeuchi, O.; Akira, S. Innate immunity to virus infection. *Immunol. Rev.* **2009**, *227*, 75–86. [CrossRef]
8. West, A.P.; Koblansky, A.A.; Ghosh, S. Recognition and signaling by toll-like receptors. *Annu. Rev. Cell Dev. Biol.* **2006**, *22*, 409–437. [CrossRef]
9. Nakahira, K.; Haspel, J.A.; Rathinam, V.A.; Lee, S.J.; Dolinay, T.; Lam, H.C.; Englert, J.A.; Rabinovitch, M.; Cernadas, M.; Kim, H.P.; et al. Autophagy proteins regulate innate immune responses by inhibiting the release of mitochondrial DNA mediated by the NALP3 inflammasome. *Nat. Immunol.* **2011**, *12*, 222–230. [CrossRef]
10. Dostert, C.; Petrilli, V.; Van Bruggen, R.; Steele, C.; Mossman, B.T.; Tschopp, J. Innate immune activation through Nalp3 inflammasome sensing of asbestos and silica. *Science* **2008**, *320*, 674–677. [CrossRef]
11. Yang, C.; Zhou, Y.; Liu, H.; Xu, P. The Role of Inflammation in Cognitive Impairment of Obstructive Sleep Apnea Syndrome. *Brain Sci.* **2022**, *12*, 1303. [CrossRef] [PubMed]
12. Feng, S.; Xu, X.; Tao, S.; Chen, T.; Zhou, L.; Huang, Y.; Yang, H.; Yuan, M.; Ding, C. Comprehensive evaluation of chemical composition and health-promoting effects with chemometrics analysis of plant derived edible oils. *Food Chem. X* **2022**, *14*, 100341. [CrossRef]
13. Vergara-Mendoza, M.; Martinez, G.R.; Blanco-Tirado, C.; Combariza, M.Y. Mass Balance and Compositional Analysis of Biomass Outputs from Cacao Fruits. *Molecules* **2022**, *27*, 3717. [CrossRef] [PubMed]
14. Dudonne, S.; Vitrac, X.; Coutiere, P.; Woillez, M.; Merillon, J.M. Comparative study of antioxidant properties and total phenolic content of 30 plant extracts of industrial interest using DPPH, ABTS, FRAP, SOD, and ORAC assays. *J. Agric. Food. Chem.* **2009**, *57*, 1768–1774. [CrossRef]
15. Kahl, R.; Kappus, H. Toxicology of the synthetic antioxidants BHA and BHT in comparison with the natural antioxidant vitamin E. *Z Lebensm Unters Forsch* **1993**, *196*, 329–338. [CrossRef] [PubMed]
16. Hamad, G.M.; Samy, H.; Mehany, T.; Korma, S.A.; Eskander, M.; Tawfik, R.G.; El-Rokh, G.; Mansour, A.M.; Saleh, S.M.; El, S.A.; et al. Utilization of Algae Extracts as Natural Antibacterial and Antioxidants for Controlling Foodborne Bacteria in Meat Products. *Foods* **2023**, *12*, 3281. [CrossRef]
17. Whysner, J.; Wang, C.X.; Zang, E.; Iatropoulos, M.J.; Williams, G.M. Dose response of promotion by butylated hydroxyanisole in chemically initiated tumours of the rat forestomach. *Food. Chem. Toxicol.* **1994**, *32*, 215–222. [CrossRef]
18. Gao, J.; Ning, C.; Wang, M.; Wei, M.; Ren, Y.; Li, W. Structural, antioxidant activity, and stability studies of jellyfish collagen peptide-calcium chelates. *Food Chem. X* **2024**, *23*, 101706. [CrossRef]
19. Lingiardi, N.; Morais, N.S.; Rodrigues, V.M.; Moreira, S.; Galante, M.; Spelzini, D.; de Assis, C.F.; de Sousa, J.F. Quinoa protein-based Buriti oil nanoparticles: Enhancement of antioxidant activity and inhibition of digestive enzymes. *Food Res. Int.* **2025**, *214*, 116693. [CrossRef]
20. Guo, Z.; Lai, J.; Wu, Y.; Fang, S.; Liang, X. Investigation on Antioxidant Activity and Different Metabolites of Mulberry (*Morus* spp.) Leaves Depending on the Harvest Months by UPLC-Q-TOF-MS with Multivariate Tools. *Molecules* **2023**, *28*, 1947. [CrossRef]
21. Shan, Y.; Sun, C.; Li, J.; Shao, X.; Wu, J.; Zhang, M.; Yao, H.; Wu, X. Characterization of Purified Mulberry Leaf Glycoprotein and Its Immunoregulatory Effect on Cyclophosphamide-Treated Mice. *Foods* **2022**, *11*, 2034. [CrossRef] [PubMed]
22. Ye, S.; Zhang, X.; Ling, G.; Xiao, X.; Huang, D.; Chen, M. A Meta-Analysis of Randomized Clinical Trials of Runzao Zhiyang Capsule in Chronic Urticaria. *Evid.-Based Complement Altern. Med.* **2022**, *2022*, 1904598. [CrossRef]
23. Cao, J.; Lai, L.; Liang, K.; Wang, Y.; Wang, J.; Yu, P.; Cao, F.; Su, E. Exploring Sustainable Protein Alternatives: Physicochemical and Functional Properties of Paper Mulberry (*Broussonetia papyrifera* (Linn.) L'Her. ex Vent.) Proteins. *Food Biophys.* **2025**, *20*, 78. [CrossRef]
24. Chen, R.; Zhou, X.; Deng, Q.; Yang, M.; Li, S.; Zhang, Q.; Sun, Y.; Chen, H. Extraction, structural characterization and biological activities of polysaccharides from mulberry leaves: A review. *Int. J. Biol. Macromol.* **2024**, *257*, 128669. [CrossRef]
25. Sun, C.; Shan, Y.; Tang, X.; Han, D.; Wu, X.; Wu, H.; Hosseininezhad, M. Effects of enzymatic hydrolysis on physicochemical property and antioxidant activity of mulberry (*Morus atropurpurea* Roxb.) leaf protein. *Food Sci. Nutr.* **2021**, *9*, 5379–5390. [CrossRef]

26. Sun, C.; Tang, X.; Shao, X.; Han, D.; Zhang, H.; Shan, Y.; Gooneratne, R.; Shi, L.; Wu, X.; Hosseininezhad, M. Mulberry (*Morus atropurpurea* Roxb.) leaf protein hydrolysates ameliorate dextran sodium sulfate-induced colitis via integrated modulation of gut microbiota and immunity. *J. Funct. Foods* **2021**, *84*, 104575. [CrossRef]
27. Kojima, Y.; Kimura, T.; Nakagawa, K.; Asai, A.; Hasumi, K.; Oikawa, S.; Miyazawa, T. Effects of Mulberry Leaf Extract Rich in 1-Deoxynojirimycin on Blood Lipid Profiles in Humans. *J. Clin. Biochem. Nutr.* **2010**, *47*, 155–161. [CrossRef] [PubMed]
28. Nguyen, K.V.; Ho, D.V.; Le, N.T.; Van Phan, K.; Heinamaki, J.; Raal, A.; Nguyen, H.T. Flavonoids and alkaloids from the rhizomes of *Zephyranthes ajax* Hort. and their cytotoxicity. *Sci. Rep.* **2020**, *10*, 22193. [CrossRef]
29. Megrous, S.; Zhao, X.; Al-Dalali, S.; Yang, Z. Response surface methodology and optimization of hydrolysis conditions for the in vitro calcium-chelating and hypoglycemic activities of casein protein hydrolysates prepared using microbial proteases. *J. Food Meas. Charact.* **2024**, *18*, 2549–2560. [CrossRef]
30. Jia, F.; Zhang, Y.; Wang, J.; Peng, J.; Zhao, P.; Zhang, L.; Yao, H.; Ni, J.; Wang, K. The effect of halogenation on the antimicrobial activity, antibiofilm activity, cytotoxicity and proteolytic stability of the antimicrobial peptide Jelleine-I. *Peptides* **2019**, *112*, 56–66. [CrossRef]
31. Coscueta, E.R.; Campos, D.A.; Osorio, H.; Nerli, B.B.; Pintado, M. Enzymatic soy protein hydrolysis: A tool for biofunctional food ingredient production. *Food Chem. X* **2019**, *1*, 100006. [CrossRef] [PubMed]
32. Habinshuti, I.; Nsengumuremyi, D.; Muhoza, B.; Ebenezer, F.; Yinka, A.A.; Antoine, N.M. Recent and novel processing technologies coupled with enzymatic hydrolysis to enhance the production of antioxidant peptides from food proteins: A review. *Food Chem.* **2023**, *423*, 136313. [CrossRef]
33. Zamora-Sillero, J.; Gharsallaoui, A.; Prentice, C. Peptides from Fish By-product Protein Hydrolysates and Its Functional Properties: An Overview. *Mar. Biotechnol.* **2018**, *20*, 118–130. [CrossRef] [PubMed]
34. Durak, A.; Baraniak, B.; Jakubczyk, A.; Swieca, M. Biologically active peptides obtained by enzymatic hydrolysis of Adzuki bean seeds. *Food Chem.* **2013**, *141*, 2177–2183. [CrossRef] [PubMed]
35. Bermejo-Cruz, M.; Osorio-Ruiz, A.; Rodríguez-Canto, W.; Betancur-Ancona, D.; Martínez-Ayala, A.; Chel-Guerrero, L. Antioxidant potential of protein hydrolysates from canola (*Brassica napus* L.) seeds. *Biocatal. Agric. Biotechnol.* **2023**, *50*, 102687. [CrossRef]
36. Ren, J.; Zhao, M.; Shi, J.; Wang, J.; Jiang, Y.; Cui, C.; Kakuda, Y.; Xue, S.J. Optimization of antioxidant peptide production from grass carp sarcoplasmic protein using response surface methodology. *Lwt-Food Sci. Technol.* **2008**, *41*, 1624–1632. [CrossRef]
37. Chen, Y.; Zheng, Z.; Ai, Z.; Zhang, Y.; Tan, C.P.; Liu, Y. Exploring the Antioxidant and Structural Properties of Black Bean Protein Hydrolysate and Its Peptide Fractions. *Front. Nutr.* **2022**, *9*, 884537. [CrossRef]
38. *GB/T 23527-2009*; Proteinase Preparations. The National Standardization Administration Commission: Beijing, China, 2009.
39. Monteiro, P.V.; Virupaksha, T.K.; Rao, D.R. Proteins of Italian millet: Amino acid composition, solubility fractionation and electrophoresis of protein fractions. *J. Sci. Food. Agric.* **1982**, *33*, 1072–1079. [CrossRef]
40. Nielsen, P.M.; Petersen, D.; Dambmann, C. Improved method for determining food protein degree of hydrolysis. *J. Food Sci.* **2001**, *66*, 642–646. [CrossRef]
41. Chongzhen, S. Enzymatic Preparation, Structural Identification and the Immunological Activity of Antioxidant Peptides Isolated from Mulberry Leaf Protein. Ph.D. Thesis, South China University of Technology, Guangzhou, China, 2017. [CrossRef]
42. Lowry, O.H.; Rosebrough, N.J.; Farr, A.L.; Randall, R.J. Protein measurement with the Folin phenol reagent. *J. Biol. Chem.* **1951**, *193*, 265–275. [CrossRef]
43. Szewczyk, A.; Marino, A.; Molinari, J.; Ekiert, H.; Miceli, N. Phytochemical Characterization, and Antioxidant and Antimicrobial Properties of Agitated Cultures of Three Rue Species: *Ruta chalepensis*, *Ruta corsica*, and *Ruta graveolens*. *Antioxidants* **2022**, *11*, 592. [CrossRef] [PubMed]
44. Chaturvedi, R.; Singha, P.K.; Dey, S. Water soluble bioactives of nacre mediate antioxidant activity and osteoblast differentiation. *PLoS ONE* **2013**, *8*, e84584. [CrossRef] [PubMed]
45. Luo, Y.; Peng, B.; Wei, W.; Tian, X.; Wu, Z. Antioxidant and Anti-Diabetic Activities of Polysaccharides from Guava Leaves. *Molecules* **2019**, *24*, 1343. [CrossRef]
46. Zhou, Y.; Zhang, R.; Wang, J.; Tong, Y.; Zhang, J.; Li, Z.; Zhang, H.; Abbas, Z.; Si, D.; Wei, X. Isolation, Characterization, and Functional Properties of Antioxidant Peptides from Mulberry Leaf Enzymatic Hydrolysates. *Antioxidants* **2024**, *13*, 854. [CrossRef]
47. Dhawan, U.; Lee, C.H.; Huang, C.C.; Chu, Y.H.; Huang, G.S.; Lin, Y.R.; Chen, W.L. Topological control of nitric oxide secretion by tantalum oxide nanodot arrays. *J. Nanobiotechnol.* **2015**, *13*, 79. [CrossRef] [PubMed]
48. Wu, X.; Zhang, Q.; Guo, Y.; Zhang, H.; Guo, X.; You, Q.; Wang, L. Methods for the Discovery and Identification of Small Molecules Targeting Oxidative Stress-Related Protein-Protein Interactions: An Update. *Antioxidants* **2022**, *11*, 619. [CrossRef]
49. Zhuang, Y.; Wu, H.; Wang, X.; He, J.; He, S.; Yin, Y. Resveratrol Attenuates Oxidative Stress-Induced Intestinal Barrier Injury through PI3K/Akt-Mediated Nrf2 Signaling Pathway. *Oxidative Med. Cell. Longev.* **2019**, *2019*, 7591840. [CrossRef]
50. Liu, M.; Wang, J.; He, Y. The U-Shaped Association between Bilirubin and Diabetic Retinopathy Risk: A Five-Year Cohort Based on 5323 Male Diabetic Patients. *J. Diabetes Res.* **2018**, *2018*, 4603087. [CrossRef]
51. Nezu, M.; Suzuki, N. Roles of Nrf2 in Protecting the Kidney from Oxidative Damage. *Int. J. Mol. Sci.* **2020**, *21*, 2951. [CrossRef]

52. Sato, Y.; Yanagita, M. Renal anemia: From incurable to curable. *Am. J. Physiol.-Renal Physiol.* **2013**, *305*, F1239–F1248. [CrossRef]
53. Heistad, D.D. Oxidative stress and vascular disease—2005 Duff Lecture. *Arterioscler. Thromb. Vasc. Biol.* **2006**, *26*, 689–695. [CrossRef] [PubMed]
54. Deng, W.; Liu, K.; Cao, S.; Sun, J.; Zhong, B.; Chun, J. Chemical Composition, Antimicrobial, Antioxidant, and Antiproliferative Properties of Grapefruit Essential Oil Prepared by Molecular Distillation. *Molecules* **2020**, *25*, 217. [CrossRef]
55. Pan, X.; Zhao, Y.; Cheng, T.; Zheng, A.; Ge, A.; Zang, L.; Xu, K.; Tang, B. Monitoring NAD(P)H by an ultrasensitive fluorescent probe to reveal reductive stress induced by natural antioxidants in HepG2 cells under hypoxia. *Chem. Sci.* **2019**, *10*, 8179–8186. [CrossRef]
56. Woo, M.; Kim, M.; Noh, J.S.; Park, C.H.; Song, Y.O. Preventative activity of kimchi on high cholesterol diet-induced hepatic damage through regulation of lipid metabolism in LDL receptor knockout mice. *Food Sci. Biotechnol.* **2018**, *27*, 211–218. [CrossRef]
57. Kishimoto, Y.; Yoshida, H.; Kondo, K. Potential Anti-Atherosclerotic Properties of Astaxanthin. *Mar. Drugs* **2016**, *14*, 35. [CrossRef]
58. Sun, C.; Tang, X.; Ren, Y.; Wang, E.; Shi, L.; Wu, X.; Wu, H. Novel Antioxidant Peptides Purified from Mulberry (*Morus atropurpurea* Roxb.) Leaf Protein Hydrolysates with Hemolysis Inhibition Ability and Cellular Antioxidant Activity. *J. Agric. Food. Chem.* **2019**, *67*, 7650–7659. [CrossRef] [PubMed]
59. Sun, C.; Wu, W.; Ma, Y.; Min, T.; Lai, F.; Wu, H. Physicochemical, functional properties, and antioxidant activities of protein fractions obtained from mulberry (*Morus atropurpurea* roxb.) leaf. *Int. J. Food Prop.* **2018**, *20*, S3311–S3325. [CrossRef]
60. Sun, C.; Wu, W.; Yin, Z.; Fan, L.; Ma, Y.; Lai, F.; Wu, H. Effects of simulated gastrointestinal digestion on the physicochemical properties, erythrocyte haemolysis inhibitory ability and chemical antioxidant activity of mulberry leaf protein and its hydrolysates. *Int. J. Food Sci. Technol.* **2018**, *53*, 282–295. [CrossRef]
61. Fan, J.; Gao, A.; Zhan, C.; Jin, Y. Degradation of soybean meal proteins by wheat malt endopeptidase and the antioxidant capacity of the enzymolytic products. *Front. Nutr.* **2023**, *10*, 1138664. [CrossRef] [PubMed]
62. Zhao, W.; Li, J.; Li, Y.; Chen, Y.; Jin, H. Preventive Effect of Collagen Peptides from Acaudina molpadioides on Acute Kidney Injury through Attenuation of Oxidative Stress and Inflammation. *Oxidative Med. Cell. Longev.* **2022**, *2022*, 8186838. [CrossRef]
63. Bavaro, T.; Cattaneo, G.; Serra, I.; Benucci, I.; Pregnolato, M.; Terreni, M. Immobilization of Neutral Protease from *Bacillus subtilis* for Regioselective Hydrolysis of Acetylated Nucleosides: Application to Capecitabine Synthesis. *Molecules* **2016**, *21*, 1621. [CrossRef] [PubMed]
64. Duijsens, D.; Palchen, K.; Verkempinck, S.; Guevara-Zambrano, J.; Hendrickx, M.; Van Loey, A.; Grauwet, T. Size exclusion chromatography to evaluate in vitro proteolysis: A case study on the impact of microstructure in pulse powders. *Food Chem.* **2023**, *418*, 135709. [CrossRef]
65. Yi, J.; Zhang, Y.; Yokoyama, W.; Liang, R.; Zhong, F. Glycation inhibits trichloroacetic acid (TCA)-induced whey protein precipitation. *Eur. Food Res. Technol.* **2015**, *240*, 847–852. [CrossRef]
66. Michalczyk, M.; Surowka, K. Changes in protein fractions of rainbow trout (*Oncorhynchus mykiss*) gravads during production and storage. *Food Chem.* **2007**, *104*, 1006–1013. [CrossRef]
67. Wu, W.; Zhang, M.; Sun, C.; Brennan, M.; Li, H.; Wang, G.; Lai, F.; Wu, H. Enzymatic preparation of immunomodulatory hydrolysates from defatted wheat germ (*Triticum vulgare*) globulin. *Int. J. Food Sci. Technol.* **2016**, *51*, 2556–2566. [CrossRef]
68. Ao, X.L.; Yu, X.; Wu, D.T.; Li, C.; Zhang, T.; Liu, S.L.; Chen, S.J.; He, L.; Zhou, K.; Zou, L.K. Purification and characterization of neutral protease from *Aspergillus oryzae* Y1 isolated from naturally fermented broad beans. *AMB Express* **2018**, *8*, 96. [CrossRef]
69. Wang, J.; Tang, Y.; Zhao, X.; Ding, Z.; Ahmat, M.; Si, D.; Zhang, R.; Wei, X. Molecular hybridization modification improves the stability and immunomodulatory activity of TP5 peptide. *Front. Immunol.* **2024**, *15*, 1472839. [CrossRef]
70. Wei, X.; Zhang, L.; Yang, Y.; Hou, Y.; Xu, Y.; Wang, Z.; Su, H.; Han, F.; Han, J.; Liu, P.; et al. LL-37 transports immunoreactive cGAMP to activate STING signaling and enhance interferon-mediated host antiviral immunity. *Cell Rep.* **2022**, *39*, 110880. [CrossRef]
71. Wang, J.; Zhou, Y.; Zhang, J.; Tong, Y.; Abbas, Z.; Zhao, X.; Li, Z.; Zhang, H.; Chen, S.; Si, D.; et al. Peptide TaY Attenuates Inflammatory Responses by Interacting with Myeloid Differentiation 2 and Inhibiting NF-kappaB Signaling Pathway. *Molecules* **2024**, *29*, 4843. [CrossRef]
72. Kim, G.N.; Jang, H.D. Flavonol content in the water extract of the mulberry (*Morus alba* L.) leaf and their antioxidant capacities. *J. Food Sci.* **2011**, *76*, C869–C873. [CrossRef]
73. Pacheco, A.F.C.; Pacheco, F.C.; Cunha, J.S.; Nalon, G.A.; Gusmão, J.V.F.; Santos, F.R.D.; Andressa, I.; Paiva, P.H.C.; Tribst, A.A.L.; Leite Junior, B.R.D.C. Physicochemical Properties and In Vitro Antioxidant Activity Characterization of Protein Hydrolysates Obtained from Pumpkin Seeds Using Conventional and Ultrasound-Assisted Enzymatic Hydrolysis. *Foods* **2025**, *14*, 782. [CrossRef] [PubMed]
74. Magalhaes, I.S.; Guimaraes, A.; Tribst, A.; Oliveira, E.B.; Leite, J.B. Ultrasound-assisted enzymatic hydrolysis of goat milk casein: Effects on hydrolysis kinetics and on the solubility and antioxidant activity of hydrolysates. *Food Res. Int.* **2022**, *157*, 111310. [CrossRef] [PubMed]

75. Mirzaee, H.; Ahmadi, G.H.; Nikoo, M.; Udenigwe, C.C.; Khodaiyan, F. Relation of amino acid composition, hydrophobicity, and molecular weight with antidiabetic, antihypertensive, and antioxidant properties of mixtures of corn gluten and soy protein hydrolysates. *Food Sci. Nutr.* **2023**, *11*, 1257–1271. [CrossRef]
76. Billi, M.; Pagano, S.; Pancrazi, G.L.; Valenti, C.; Bruscoli, S.; Di Michele, A.; Febo, M.; Grignani, F.; Marinucci, L. DNA damage and cell death in human oral squamous cell carcinoma cells: The potential biological effects of cannabidiol. *Arch. Oral Biol.* **2024**, *169*, 106110. [CrossRef] [PubMed]
77. Cai, Y.; Prochazkova, M.; Kim, Y.S.; Jiang, C.; Ma, J.; Moses, L.; Martin, K.; Pham, V.; Zhang, N.; Highfill, S.L.; et al. Assessment and comparison of viability assays for cellular products. *Cytotherapy* **2024**, *26*, 201–209. [CrossRef]
78. Tao, L.; Gu, F.; Liu, Y.; Yang, M.; Wu, X.Z.; Sheng, J.; Tian, Y. Preparation of antioxidant peptides from Moringa oleifera leaves and their protection against oxidative damage in HepG2 cells. *Front. Nutr.* **2022**, *9*, 1062671. [CrossRef]
79. Zheng, L.; Yu, H.; Wei, H.; Xing, Q.; Zou, Y.; Zhou, Y.; Peng, J. Antioxidative peptides of hydrolysate prepared from fish skin gelatin using ginger protease activate antioxidant response element-mediated gene transcription in IPEC-J2 cells. *J. Funct. Foods* **2018**, *51*, 104–112. [CrossRef]
80. Cheng, M.; Wang, H.; Hsu, K.; Hwang, J. Anti-inflammatory peptides from enzymatic hydrolysates of tuna cooking juice. *Food Agric. Immunol.* **2015**, *26*, 770–781. [CrossRef]
81. Fedchenko, V.; Morozevich, G.; Medvedev, A. The effect of renalase-derived peptides on viability of HepG2 and PC3 cells. *Biomeditsinskaia Khimiia* **2023**, *63*, 184–187. [CrossRef]
82. Chen, Q.; Yu, M.; Tian, Z.; Cui, Y.; Deng, D.; Rong, T.; Liu, Z.; Song, M.; Li, Z.; Ma, X.; et al. Exogenous Glutathione Protects IPEC-J2 Cells against Oxidative Stress through a Mitochondrial Mechanism. *Molecules* **2022**, *27*, 2416. [CrossRef]
83. Akturk, A. Enrichment of Cellulose Acetate Nanofibrous Scaffolds with Retinyl Palmitate and Clove Essential Oil for Wound Healing Applications. *Acs Omega* **2023**, *8*, 5553–5560. [CrossRef] [PubMed]
84. Anand, S.; Rajinikanth, P.S.; Arya, D.K.; Pandey, P.; Gupta, R.K.; Sankhwar, R.; Chidambaram, K. Multifunctional Biomimetic Nanofibrous Scaffold Loaded with Asiaticoside for Rapid Diabetic Wound Healing. *Pharmaceutics* **2022**, *14*, 273. [CrossRef]
85. Butzbach, K.; Konhauser, M.; Fach, M.; Bamberger, D.N.; Breitenbach, B.; Epe, B.; Wich, P.R. Receptor-mediated Uptake of Folic Acid-functionalized Dextran Nanoparticles for Applications in Photodynamic Therapy. *Polymers* **2019**, *11*, 896. [CrossRef]
86. Duan, Z.; Yuan, C.; Han, Y.; Zhou, L.; Zhao, J.; Ruan, Y.; Chen, J.; Ni, M.; Ji, X. TMT-based quantitative proteomics analysis reveals the attenuated replication mechanism of Newcastle disease virus caused by nuclear localization signal mutation in viral matrix protein. *Virulence* **2020**, *11*, 607–635. [CrossRef] [PubMed]
87. Chen, X.; Yan, L.; Guo, Z.; Chen, Z.; Chen, Y.; Li, M.; Huang, C.; Zhang, X.; Chen, L. Adipose-derived mesenchymal stem cells promote the survival of fat grafts via crosstalk between the Nrf2 and TLR4 pathways. *Cell Death Dis.* **2016**, *7*, e2369. [CrossRef]
88. Xu, W.; Wang, M.; Cui, G.; Li, L.; Jiao, D.; Yao, B.; Xu, K.; Chen, Y.; Long, M.; Yang, S.; et al. Astaxanthin Protects OTA-Induced Lung Injury in Mice through the Nrf2/NF-kappaB Pathway. *Toxins* **2019**, *11*, 540. [CrossRef] [PubMed]
89. Paramo, T.; Tomasio, S.M.; Irvine, K.L.; Bryant, C.E.; Bond, P.J. Energetics of Endotoxin Recognition in the Toll-Like Receptor 4 Innate Immune Response. *Sci. Rep.* **2015**, *5*, 17997. [CrossRef]
90. Kaewin, S.; Changsorn, K.; Sungkaworn, T.; Hiranmartsuwan, P.; Yaosanit, W.; Rukachaisirikul, V.; Muanprasat, C. Fungus-Derived 3-Hydroxyterphenyllin and Candidusin A Ameliorate Palmitic Acid-Induced Human Podocyte Injury via Anti-Oxidative and Anti-Apoptotic Mechanisms. *Molecules* **2022**, *27*, 2109. [CrossRef]
91. Chunhakant, S.; Chaicharoenpong, C. Antityrosinase, Antioxidant, and Cytotoxic Activities of Phytochemical Constituents from *Manilkara zapota* L. *Bark. Molecules* **2019**, *24*, 2798. [CrossRef]
92. Dhall, S.; Hoffman, T.; Sathyamoorthy, M.; Lerch, A.; Jacob, V.; Moorman, M.; Kuang, J.Q.; Danilkovitch, A. A Viable Lyopreserved Amniotic Membrane Modulates Diabetic Wound Microenvironment and Accelerates Wound Closure. *Adv. Wound Care* **2019**, *8*, 355–367. [CrossRef]
93. Rosenfeld, Y.; Shai, Y. Lipopolysaccharide (Endotoxin)-host defense antibacterial peptides interactions: Role in bacterial resistance and prevention of sepsis. *Biochim Biophys Acta* **2006**, *1758*, 1513–1522. [CrossRef] [PubMed]
94. Spinaci, A.; Lambertucci, C.; Buccioni, M.; Dal Ben, D.; Graiff, C.; Barbalace, M.C.; Hrelia, S.; Angeloni, C.; Tayebati, S.K.; Ubaldi, M.; et al. A(2A) Adenosine Receptor Antagonists: Are Triazolotriazine and Purine Scaffolds Interchangeable? *Molecules* **2022**, *27*, 2386. [CrossRef]
95. Kim, D.G.; Choi, J.W.; Jo, I.J.; Kim, M.J.; Lee, H.S.; Hong, S.H.; Song, H.J.; Bae, G.S.; Park, S.J. Berberine ameliorates lipopolysaccharide-induced inflammatory responses in mouse inner medullary collecting duct-3 cells by downregulation of NF-kappaB pathway. *Mol. Med. Rep.* **2020**, *21*, 258–266. [CrossRef] [PubMed]
96. Ryan, K.A.; Smith, M.J.; Sanders, M.K.; Ernst, P.B. Reactive oxygen and nitrogen species differentially regulate Toll-like receptor 4-mediated activation of NF-kappa B and interleukin-8 expression. *Infect. Immun.* **2004**, *72*, 2123–2130. [CrossRef] [PubMed]
97. Gambuzza, M.; Licata, N.; Palella, E.; Celi, D.; Foti, C.V.; Italiano, D.; Marino, S.; Bramanti, P. Targeting Toll-like receptors: Emerging therapeutics for multiple sclerosis management. *J. Neuroimmunol.* **2011**, *239*, 1–12. [CrossRef]

98. Diao, J.; Miao, X.; Chen, H. Anti-inflammatory effects of mung bean protein hydrolysate on the lipopolysaccharide- induced RAW264.7 macrophages. *Food Sci. Biotechnol.* **2022**, *31*, 849–856. [CrossRef]
99. Song, T.; Zhou, M.; Li, W.; Lv, M.; Zheng, L.; Zhao, M. The anti-inflammatory effect of vasoactive peptides from soybean protein hydrolysates by mediating serum extracellular vesicles-derived miRNA-19b/CYLD/TRAF6 axis in the vascular microenvironment of SHRs. *Food Res. Int.* **2022**, *160*, 111742. [CrossRef]

Disclaimer/Publisher's Note: The statements, opinions and data contained in all publications are solely those of the individual author(s) and contributor(s) and not of MDPI and/or the editor(s). MDPI and/or the editor(s) disclaim responsibility for any injury to people or property resulting from any ideas, methods, instructions or products referred to in the content.